

## Development of novel composites of incompatible barrier polymers and their optimal processing conditions for recyclable thermoformable food packaging sheet

AKIKI Alain<sup>1,2,a\*</sup>, EL RASSY Elissa<sup>2</sup>, CHALLITA Georges<sup>3</sup>,  
NACCOUL Rouaida Abou<sup>1</sup>, BAILLEUL Jean-Luc<sup>2</sup>

<sup>1</sup>INDEVCO PACT, Christ le Roi, Industrial Zone, Zouk Mosbeh P.O.BOX :11-2354, Lebanon

<sup>2</sup>Nantes Université, UMR CNRS 6607, LTEN, Rue Christian Pauc, 44300 Nantes, France

<sup>3</sup>Lebanese University, Faculty of Engineering, Roumieh, Lebanon

<sup>a</sup>alain.akiki@etu.univ-nantes.fr

**Keywords:** Dispersed Nanophase, MXD6, Compatibilizer, Thermoplastic Composite, Lamellar Morphology, Permeability

**Abstract.** In this work, a high barrier polymer MXD6 (m-xylene diamine) has been incorporated in a PE (polyethylene) matrix to create an extensible, thermoplastic composite system. MXD6 is a high barrier and glassy polymer. However, being polar, it is incompatible with a non-polar PE. To this date, there were no significant attempts neither in compatibilizing a binary blend of PE/MXD6 nor in exploring the benefits of orientation on such a mixed system. The main value proposition in this work resides in reducing the dispersed MXD6 phase close to a submicron scale in the PE matrix by designing an adequate mixing process/compatibilizer method. Thermal characterization of the composites and the scanning electron microscopy have confirmed that the MXD6 dispersed phase in the compatibilized blends has been physically and thermally confined; its crystallization during cooling stage has been inhibited. The compatibilized blend shows a creation of an interface adhesion between phases. The dispersed phase average particle size is stabilized at around 0.5  $\mu\text{m}$  enhancing the recyclability of the final product.

### Introduction

Extensive research has been conducted to incorporate nano-minerals in a polyolefin matrix to improve its gas barrier properties in food packaging [1]. Nano minerals such as MMT (montmorillonite) and graphene can produce a long tortuous path to gas molecules if exfoliated efficiently. Although many studies yielded promising findings, such nanocomposites have limited extensibility due to the brittleness of the minerals, making it obsolete in applications such as thermally stretched films/sheets. In addition, there has been a reserved approach from food packers towards using nano-minerals in packaging due to food contamination risks [2].

A new concept has emerged recently in dispersing high barrier polymers in a polyolefin continuous matrix. The idea is to reduce the particle size of the dispersed phase to reach the order of nano-minerals, and then convert the thermoplastic composite into films or sheets by extrusion. In a scope extending beyond this paper and interpreted in Fig.1, we propose stretching such sheets to realize a lamellar morphology and thus create a long tortuous path for gas molecules.



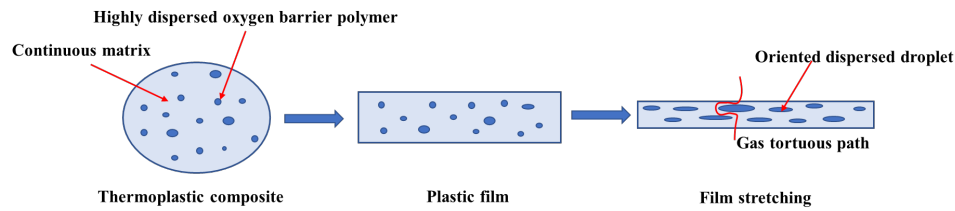


Fig.1 Realization model concept of the extended study

In this study, we have selected a special polyamide called MXD6 (m-xylene diamine) as the dispersed phase. This polymer has a very high barrier to gas, specifically oxygen, even at high relative humidity (RH %). The chemical structure in Fig.2 illustrates a molecule with an aromatic ring which is the reason behind its high glass transition temperature  $T_g$  around 87 °C. MXD6 is a glassy polymer, therefore is only stretchable above its  $T_g$ .

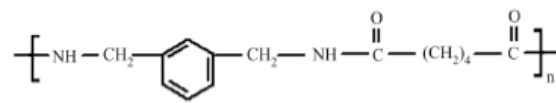


Fig.2 Molecular structure of MXD6

We used a linear low-density polyethylene (LLDPE) as the continuous phase (matrix). LLDPE is known for its extensibility, toughness, good thermal welding at relatively low temperatures (90-120 °C). LLDPE is also known to be a medium barrier to moisture.

MXD6 and LLDPE have been used in the past in multilayer extrusion technology to produce high barrier films [3]. However, such films are non-recyclable, and the production technology requires huge investments and has relatively high operational challenges compared to our concept that requires fewer numbers of layers.

The novelty in our study resides in investigating the following aspects:

- The thermoplastic composites can be extruded in simple existing technologies of 1 to 3 layers.
- To this date, no significant attempts neither in compatibilizing a binary blend of PE/MXD6 nor in exploring the benefits of orientation on such a mixed system. The main value proposition in this work resides in achieving a dispersed MXD6 nanophase in a PE matrix by designing an adequate mixing process-compatibilizer method.
- A compatibilized thermoplastic composite can be recycled.

In this paper, we will focus on the thermal characterization of the thermoplastic composites. We will also show the efficiency of compatibilization as well as its impact on the thermal transitions and the morphology of the composites.

## Materials

A LLDPE having a density 0.918 g/cm<sup>3</sup> and a melt flow index of 3.5 g/10 min was selected as the continuous matrix. This polymer has a relatively high toughness and stretchability compared to other semi-crystalline polymers. However most importantly, it is thermally weldable at relatively low temperatures ranging between 100 and 120 °C. The needed properties were excerpted from the material specification sheets provided by the suppliers and have been tabulated in table 1.

Table 1. Major properties of selected LLDPE & MXD6 grades

Material	Melt flow index [g/10 min]	Melt Viscosity [Pa.s]	Density [g/cm <sup>3</sup> ]	Melting peak [°C]	Tg [°C]
LLDPE	3.5*	NA	0.918	118	-
MXD6	2.0**	770/300 ***	1.22	237	85

\* @190 °C/2.16 kg    \*\* @275 °C/0.325 kg    \*\*\*@260 °C 100/1000 s<sup>-1</sup>

Thermoplastic composites made of LLDPE and different concentrations of MXD6 were prepared. The composites were prepared using a lab scale co-rotating twin screw extruder with L/D=44 and screws diameter of 22 mm. The temperatures profile was set at 240-260 °C to exceed the peak melting temperature of MXD6.

A highly grafted maleic anhydride grafted LLDPE (MAH-g-PE) thereof called MAH-GC was added at different weight % to compatibilize the continuous LLDPE matrix with the MXD6 dispersed phase. The formulations of the thermoplastic composites, with and without compatibilizers, and their respective names are detailed in table 2.

Table 2. Thermoplastic composites studied in this article.

Compatibilizer	Compatibilizer weight %	Composite Name	Formulation PE/MXD6/Comp
None	0	MX10	90/10/0
		MX20	80/20/0
		MX30	70/30/0
MAH-g-LLDPE	3	MX20-GC3	77/20/3
	5	MX20-GC5	75/20/5
	7	MX20-GC7	73/20/7

### Methods & Experimental Characterization

Before preparing the compounds in the twin screw extruder, we dried the MXD6 at 110 °C for 3 hours under atmospheric pressure. The compatibilizers were dried at 50 °C for 4 hours. LLDPE being hydrophobic, does not absorb humidity and therefore did not require pre-drying. Dried samples were kept in a concealed container until extrusion.

Before characterization, the samples of thermoplastic composites were dried at 90 °C for 4 hours under atmospheric pressure. The pre-dried samples of thermoplastic composites were thermally characterized using differential scanning calorimetry (DSC). The cycles consisted of a first heating ramp from 25 °C to 300 °C at 10 °C/min, an isotherm at 300 °C for 5 min, a cooling ramp down from 300 °C to 25 °C at different cooling rates, a second isotherm at 25 °C for 5 min and a second heating ramp up from 25 °C to 300 °C at 10 °C/min. The first heating stage serves as an annealing process for the extruded samples. The cooling stage was done at 2, 3, 5, 10 and 20 °C/min cooling rates. The thermal transitions of the latter stage and the second heating stage were reported and measured in this study.

Pre-dried composites pellets were pressed at 250 °C to produce a film having a thickness average of 200 ± 5 µm. 5 sheets were prepared from each composition for repeatability. The identification of the functional groups in each sample was done by Fourier Transform Infrared (FTIR). The spectroscopy was conducted using Bruker equipment in transmission mode (FTIR-TR) with 32 scans and wavelengths ranging from 4000 to 400 cm<sup>-1</sup>. Scanning electron microscopy (SEM) was used to determine the dimensions of the dispersed phase, and to optically characterize the interfacial interaction between the MXD6 dispersed phase and PE continuous phase.

A thermogravimetric analyzer (TGA) was used to test the thermal stability of all raw material granules. Samples of (20 ± 1) mg were prepared and tested in non-isothermal mode as per test method ASTM E1131-20 at 10 °C/min heating rate in the range of 25 to 900 °C.

## Results and discussion

The DSC exothermal thermogram of MXD6 presented in Fig.3A shows that the polymer has a peak crystallization temperature at 152 °C and a  $T_g$  at 87 °C. The second heating stage shows a cold crystallization peak thermal crystallization at 145 °C which is an important thermal transition to track throughout the compounding stage. The peak melting temperature of the polymer was detected at 231 °C.

In Fig.3B LLDPE shows a peak crystallization temperature at 98 °C and two melting modes with respective peak melting temperatures at 106 °C and 116 °C. The lowest one being related to the low molecular weight portion rich in short chain branches resulting from higher distribution of C6 copolymer [7].

The thermograms of the MAH-GC compatibilizer shows that it has a peak crystallization temperature at 52 °C and a peak melting temperature at 70 °C.

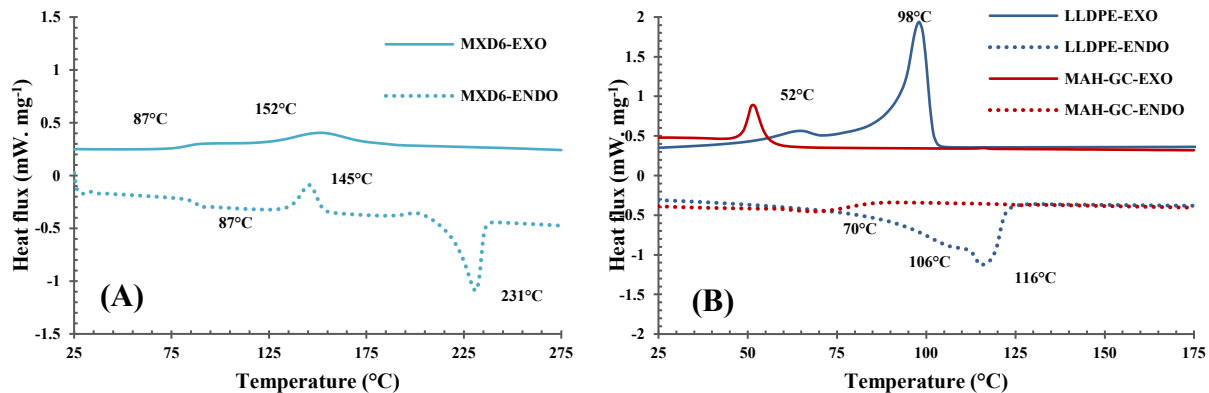


Fig 3. DSC thermograms of (A)MXD6 (B)LLDPE & MAH-GC

The crystallinity of MXD6 can be calculated from the DSC thermogram using the following formula [8]:

$$X_c = \frac{(\Delta H_f - \Delta H_{cc})}{\Delta H_f^0} = 20.2 \% \quad (1)$$

Where  $\Delta H_f = 16.39$  J/g is the measured enthalpy of fusion of MXD6,  $\Delta H_{cc} = 51.7$  J/g is the measured enthalpy of cold crystallization, and  $\Delta H_f^0 = 175$  J/g is the heat of fusion of a fully crystalline MXD6 [9].

### Thermal stability of sensitive components.

The temperature of the twin screw extrusion (TSE) mixing process and in subsequent film extrusion should exceed the end melting point of MXD6 which is  $T_{end} \sim 240$  °C as measured by DSC. We will show in a later section that the compatibilization between MXD6 and PE using a MAH-GC is a reactive process which leads to grafting the MXD6 to the MAH-GC. Accordingly, an increase in the molecular weight of the component is expected resulting in an increase in extrusion torque and therefore overheating in the extruder. Thus, instead of isothermal stability tests, we put the LLDPE and the MAH-GAC compatibilizer in a non-isothermal TGA ramp to confirm their thermal stability in the expected processing range between 250 °C and 270 °C. Indeed, Fig.4 and Table 3. show that LLDPE has undergone zero thermal decomposition whereas the compatibilizer lost less than 0.5 % of its weight making it relatively stable in this range. To note that the degradation of LLDPE due to oxidation or crosslinking has been tested by parallel plate rheology which confirmed its stability. However, this extended study remains out of the scope of this paper.

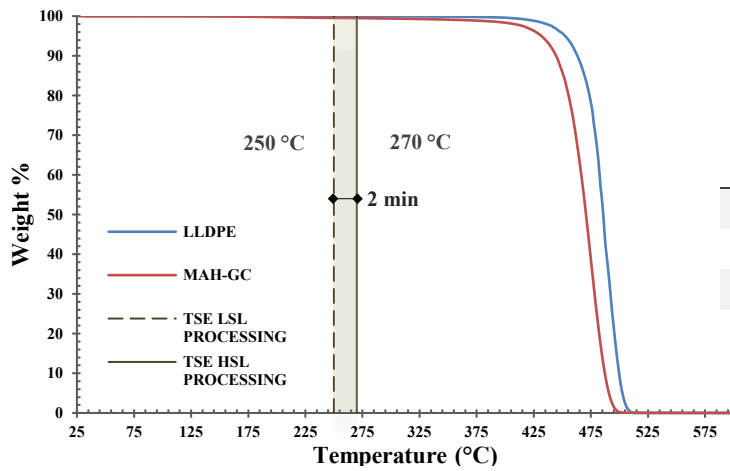


Table 3. Thermal weight loss of the compatibilizer and the LLDPE

	MAH-GC	PE
Weight loss % @ 250 °C	0.44	0
Weight loss % @ 270 °C	0.49	0
Loss % in the processing range	0.05	0

Fig 4. TGA thermogram of LLDPE & MAH-GC

Study of non-compatibilized composites.

The DSC thermograms of the thermoplastic composites at 10, 20 and 30 % of MXD6 without compatibilizers have been overlaid in Fig.5. MX10 shows only crystallization temperature related to LLDPE at around 101 °C and 65 °C but no crystallization related to MXD6 in the exothermal scan. However, a cold crystallization temperature of MXD6 at 133 °C in the endothermal scan. At the other hand, crystallization peaks of MX20 & MX30 have been detected of respectively at 178 °C and 180 °C. The increase of the crystallization peaks has been accompanied with an increase in respective melting peaks and enthalpy of fusion in the endotherm as seen in Table 4 and Fig 6.

As a first outcome, MXD6 having low and slow crystallization as shown in the previous paragraph, does not undergo crystallization in cooling stage even at a relatively slow 10 °C/min cooling rate.

At higher %, the MXD6 phase shows a separate crystallization peak from the LLDPE phase which confirms the incompatibility between phases.

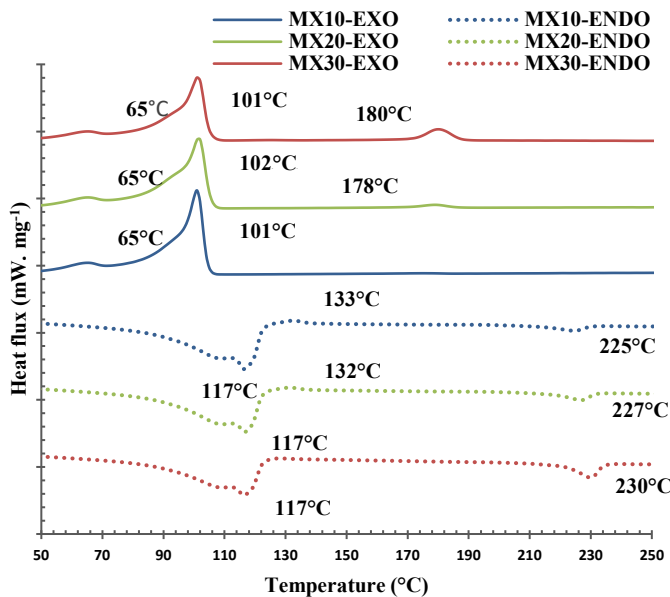


Fig 5. DSC Thermograms of MX10, MX20, MX30

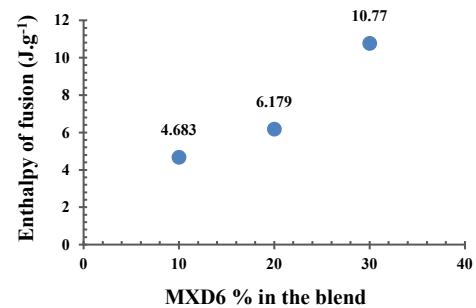


Fig 6. MXD6 Heat of fusion with MXD6 %

Table 4. Thermal transitions of non-compatibilized composites

	$T_{ep}[^{\circ}C]$	$T_{cc}[^{\circ}C]$	$T_{mp}[^{\circ}C]$	$\Delta H_f$ [J.g <sup>-1</sup> ]
MX10	ND	133	225	4.7
MX20	178	132	227	6.2
MX30	181	ND	230	10.8

The FTIR spectrum of the non-compatibilized composites have been overlaid in Fig.7. The relative absorption of the MXD6 phase increases in the same direction of the level of MXD6 in the blend. We have not detected any new absorption wavelength which means that there was no chemical reaction between phases. Fig 7B shows that the linear relation between the absorption units and the MXD6 weight % in the composite with a correlation factor of 0.9925. The latter confirms the precise weight % of MXD6 in the blends.

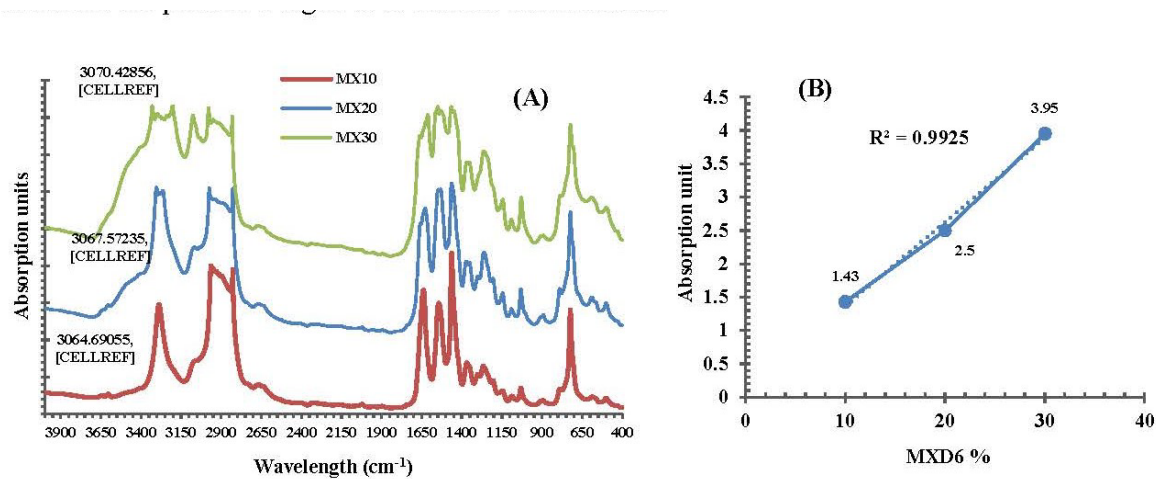


Fig 7. (A) FTIR-TR of MX10, MX20 and MX30  
 (B) Absorption of N-H(MXD6) in the range 3065-3070 cm<sup>-1</sup> vs MXD6 %

Study of compatibilized composites.

The DSC thermograms of the compatibilized composites are overlaid in Fig 9. For MAH-GC at 5 & 7 % the crystallization peak temperatures in exothermal cycle have disappeared completely. However, the related heat of fusion in the endothermal cycle are clearly detected meaning that the MXD6 dispersed phase has now a slower crystallization rate than with the non-compatibilized one. The MXD6 phase has been thermally confined, the reason behind it is the geometrical confinement which will be elaborated in later section in this study. One of the most interesting findings in this study is the existence of 2 modes of compatibilization:

- *Mode 1:* Transitional confinement of the dispersed phase at low level of MAH-GC such as 3 %. The thermogram of MX20-GC3 shows a multiple peak of crystallization in exothermal scan. In fact, such a behavior is called fractionated crystallization in semi crystalline polymers. Arnal et al. [5] have first studied this mode when mixing incompatible polymers such as polyethylene in atactic polystyrene. In fact, the heterogeneity of the microdomains and the dispersed phase sizes have been found to be the reason behind this matter. Indeed, Wang et al. [6] have made a detailed elaboration on this behavior and they found as we quote:

*“When the crystallizing polymer is divided into numerous MDs (microdomains), such as droplets dispersed in a liquid medium or in a matrix of an immiscible polymer, fractionated crystallization can arise.”*

The illustration of the concept is present in Fig 8 where A, B, C & D represent different nucleating sites in a polymer blend containing microdomains such as MXD6 in our case.

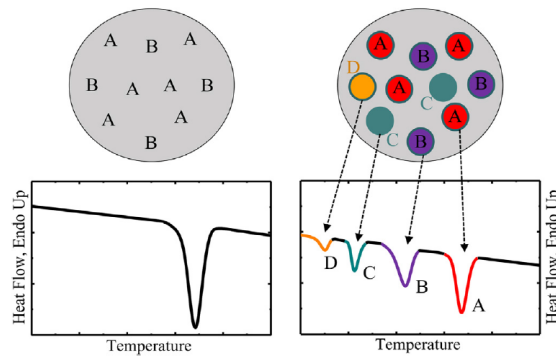


Fig 8. Concept of fractionated crystallization illustrated by Wang et al. [6]

- *Mode2*: Steady-state confinement where the dispersed phase is confined homogeneously, in a later section we will confirm that this is related to a narrow distribution of a reduced dispersed particle sizes. At 5 % & 7 % of MAH-GC, we can see the disappearance of crystallization peaks and the  $\Delta H_f$  of the MXD6 phases is in both cases around 9 J/g. The latter is described in Fig 10.

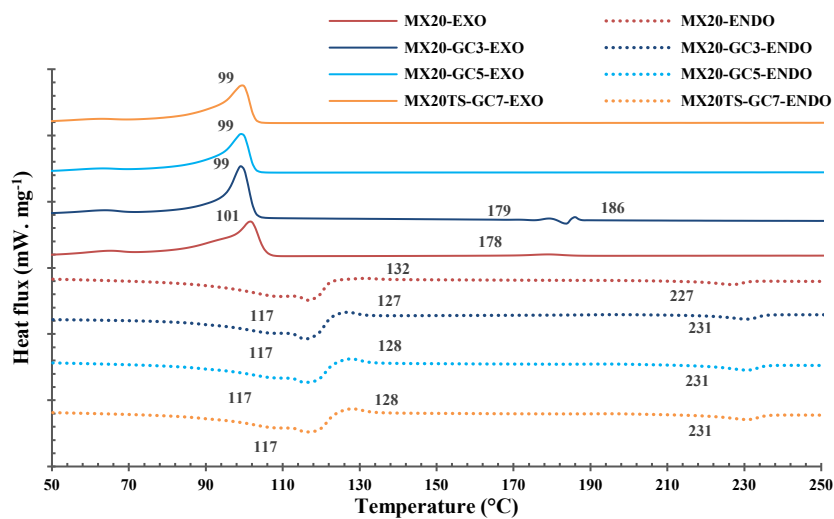


Fig 9. DSC Thermograms of MX20, MX20-GC3, MX20-GC5 & MX20GC7

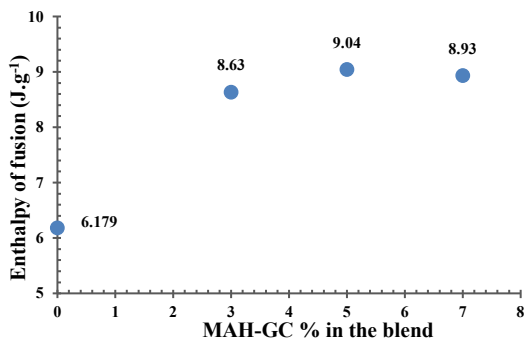


Fig 10. MXD6 Heat of fusion with MAH-GC %

Table 5. Thermal transitions of compatibilized composites

	$T_{cp}$ [°C]	$T_{cc}$ [°C]	$T_{mp}$ [°C]	$\Delta H_f$ [J/g]
MX20	178	132	227	6.2
MX20-GC3	179/186	127	231	8.6
MX20-GC5	ND	128	231	9.0
MX20-GC7	ND	128	231	8.9

The FTIR spectrum of the compatibilized composites are overlaid in Fig.11. We have detected a new functional group at  $1787\text{ cm}^{-1}$  which was not present in the non-compatibilized MX20 (cf. Fig.11A). This wavelength is related to the asymmetric C=O stretching in the MAH group present in the compatibilizer [13]. The absorption of this functional group increases with the % of MAH-GC confirming the incremental level of the compatibilizer as intended in the blend as shown in Fig.11B. The latter confirms the precise weight % of MAH-GC in the blend.

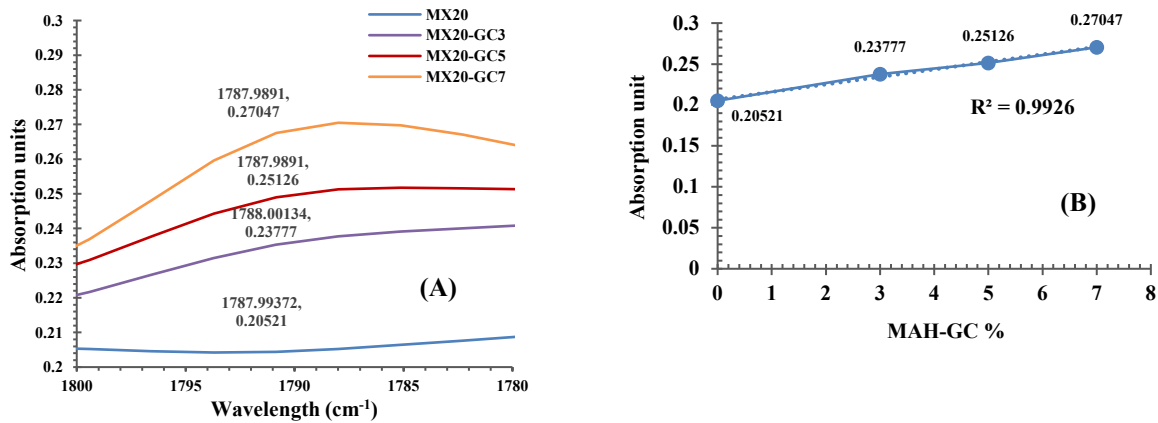


Fig 11. (A) Overlay FTIR-TR of wavelength range  $1800\text{-}1780\text{ cm}^{-1}$   
 (B) Absorption units @  $1788\text{ cm}^{-1}$  (MAH) vs MAH-GC %

### Effect of compatibilization on the morphology of the composites

The morphology tested by SEM of MX20 and MX20-GC7 blends are displayed in Fig.12. The compatibilized blend shows a significant reduction of the dispersed MXD6 size. MXD6 phase has been dispersed in MX20 with sizes reaching  $4\text{ }\mu\text{m}$  whereas the droplets size in the MX20-GC7 is mainly below  $1\text{ }\mu\text{m}$ . In addition, the MXD6 droplets in MX20 is completely separated from the LLDPE phase, whereas there is a significant interface adhesion (a typical adhesion area in red circle) between the droplets and LLDPE in MX20-GC7.

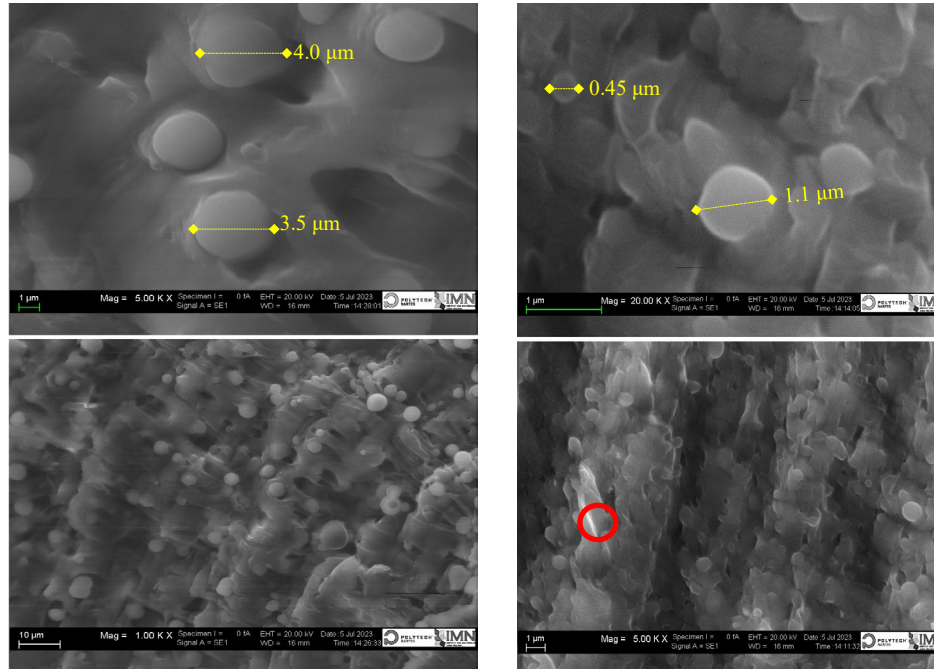


Fig 12. SEM microscopy of MX20(Left), MX20-GC7(Right)

It is very important to note that this interface adhesion is the reason behind the physical and thermal confinement. The droplet size is directly related to the interfacial tension between phases as per the Taylor’s formula [10,11,12]

$$R_{min} = \frac{2^{-\frac{1}{2}} Ca_{crit} \cdot \Gamma}{\eta_m \cdot \dot{\gamma}} \quad (2)$$

Where  $R_{min}$  is the minimum theoretical droplet radius,  $\Gamma$  is the interfacial tension between phases,  $\eta_m$  is the matrix viscosity and  $\dot{\gamma}$  is the mixing shear rate. the critical capillary number  $Ca_{crit}$  can be retrieved from Grace’s curve [10,11,12]. We deduce that the compatibilizer has created an interfacial bond between phase therefore reducing the interfacial tension which was the reason behind the confinement of the MXD6 droplets in the compatibilized composites. The second finding is that selected MAH-GC is an efficient compatibilizer between LLDPE & MXD6.

**Summary**

An important outcome of this study is that compatibilization of LLDPE and MXD6 mixed in a twin-screw extruder using 5 to 7 % MAH-g-PE leads to a confinement of the crystallization and the droplet size of the MXD6 dispersed phase. More importantly, the confinement happens after annealing the composites in the first heating cycle in DSC, this leads to a conclusion that the droplets size will remain stable in subsequent extrusion processes which will be confirmed at a later project phase. Thus, the composite acts as a sub-micro filled LLDPE improving its recyclability in LLDPE stream.

However, additional works are still needed to complete this work, namely detecting the fractionated crystals as well as the ones in steady-state mode. The latter can be done using WAXS and XRD techniques.

## Acknowledgement

Authors want to thank IMN laboratory for allowing us the use of their SEM. We also thank INDEVCO for its financial and material support.

## References

- [1] J. Luna and A. Vílchez, “Polymer nanocomposites for food packaging,” *Emerging Nanotechnologies in Food Science*, pp. 119–147, 2017. <https://doi.org/10.1016/B978-0-323-42980-1.00007-8>
- [2] H. Onyeaka, P. Passaretti, T. Miri, and Z. T. Al-Sharif, “The safety of nanomaterials in food production and packaging,” *Current Research in Food Science*, vol. 5, pp. 763–774, 2022. <https://doi.org/10.1016/j.crfs.2022.04.005>
- [3] Fereydoon, M. (2014). Development of High Barrier Nylon Based Multilayer Films [Ph.D. thesis, École Polytechnique de Montréal]. PolyPublie.
- [4] Seif, S. (2009). Temporally programmed stretching of polymer films: Influence of nanoparticles. The University of Akron.
- [5] Arnal, M. L., Matos, M. E., Morales, R. A., Santana, O. O., & Müller, A. J. (1998). Evaluation of the fractionated crystallization of dispersed polyolefins in a polystyrene matrix. *Macromolecular Chemistry and Physics*, 199(10), 2275-2288. [https://doi.org/10.1002/\(SICI\)1521-3935\(19981001\)199:10<2275::AID-MACP2275>3.0.CO;2-#](https://doi.org/10.1002/(SICI)1521-3935(19981001)199:10<2275::AID-MACP2275>3.0.CO;2-#)
- [6] Sangroniz, L., Wang, B., Su, Y., Liu, G., Cavallo, D., Wang, D., & Müller, A. J. (2021). Fractionated crystallization in semicrystalline polymers. *Progress in Polymer Science*, 115, 101376. <https://doi.org/10.1016/j.progpolymsci.2021.101376>
- [7] Mariangela Camargo, Maria Madalena Camargo Forte & Carlos Rodolfo Wolf (2008): Linear Low Density Polyethylene Thermal Fractionation by DSC Technique, *International Journal of Polymer Analysis and Characterization*, 13:1, 49-65. <https://doi.org/10.1080/10236660701802593>
- [8] Kong, Y., & Hay, J. N. (2002). The measurement of the crystallinity of polymers by DSC. *Polymer*, 43(14), 3873-3878. [https://doi.org/10.1016/S0032-3861\(02\)00235-5](https://doi.org/10.1016/S0032-3861(02)00235-5)
- [9] Doudou, B., Dargent, E., & Grenet, J. (2006). Crystallization and melting behaviour of poly (m-xylene adipamide). *Journal of thermal analysis and calorimetry*, 85(2), 409-415. <https://doi.org/10.1007/s10973-005-7299-y>
- [10] Fortelný, I., & Jůza, J. (2021). The effects of copolymer compatibilizers on the phase structure evolution in polymer blends—a review. *Materials*, 14(24), 7786. <https://doi.org/10.3390/ma14247786>
- [11] Araujo, J. R., Vallim, M. R., Spinacé, M. A. S., & De Paoli, M. A. (2008). Use of postconsumer polyethylene in blends with polyamide 6: effects of the extrusion method and the compatibilizer. *Journal of applied polymer science*, 110(3), 1310-1317. <https://doi.org/10.1002/app.28441>
- [12] Chloé Épinat. Morphology development and rheological properties of reactively compatibilized Polyamide 6 / High Density Polyethylene blends. Material chemistry. Université Claude Bernard - Lyon I, 2014.
- [13] Karakus, G., Polat, Z. A., Yenidunya, A. F., Zengin, H. B., & Karakus, C. B. (2013). Synthesis, characterization and cytotoxicity of novel modified poly [(maleic anhydride)-co-(vinyl acetate)]/noradrenaline conjugate. *Polymer international*, 62(3), 492-500. <https://doi.org/10.1002/pi.4341>